

Supporting Material to
**Methyl Acrylate Polymerizations in the Presence
of a Copper/N₃S₃ Macrobicyclic Cage in DMSO
at 25 °C.**

*Craig A. Bell,^a Qiao Sun,^a Hong Zhang,^a Sean C. Smith,^a Paul V. Bernhardt,^b Michael J. Monteiro**^a

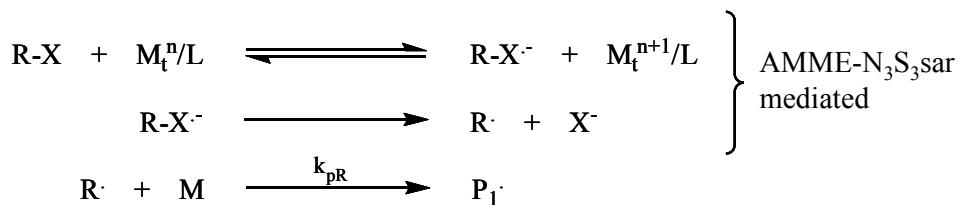
^a Australian Institute for Bioengineering and Nanotechnology, University of Queensland, Brisbane QLD 4072, Australia

^b School of Chemistry and Molecular Biosciences, University of Queensland, Brisbane QLD 4072

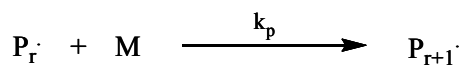
*author to whom correspondence should be sent:

e-mail: m.monteiro@uq.edu.au

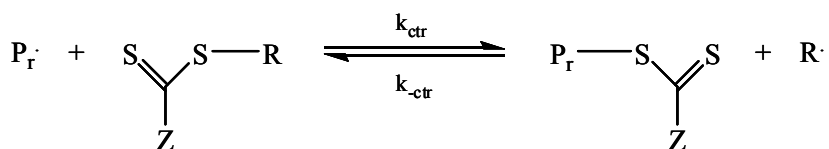
Initiation



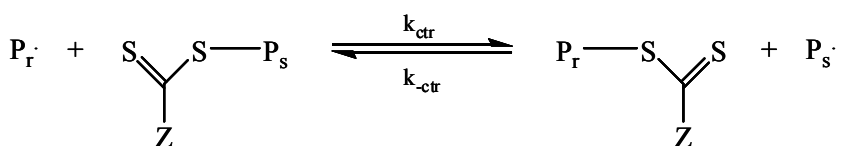
Propagation



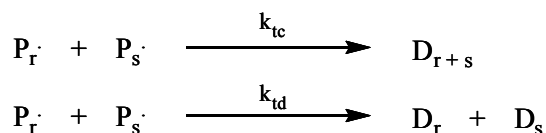
Pre-equilibrium



Main equilibrium



Termination



Scheme S1. Mechanism for AMME-N₃S₃sar mediated initiation and RAFT mediated polymerizations.

$E_{1/2}, V \text{ (vs } Fc^{+0})$

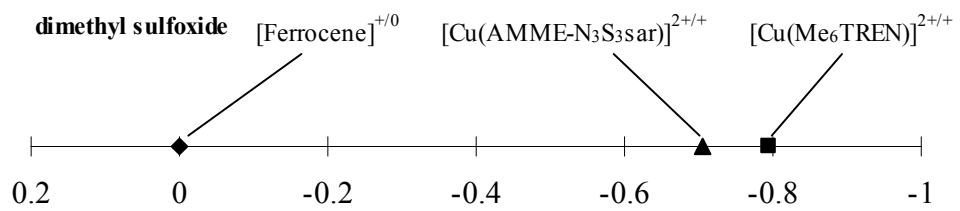


Figure S1. Redox potentials of $CuBr_2/AMME-N_3S_3sar$, $CuBr_2/Me_6TREN$ and Ferrocene in both dimethyl sulfoxide and acetonitrile. All complex concentrations are 1 mM, contain 0.1 M Et_4NClO_4 and are referenced to Fc^{+0} .

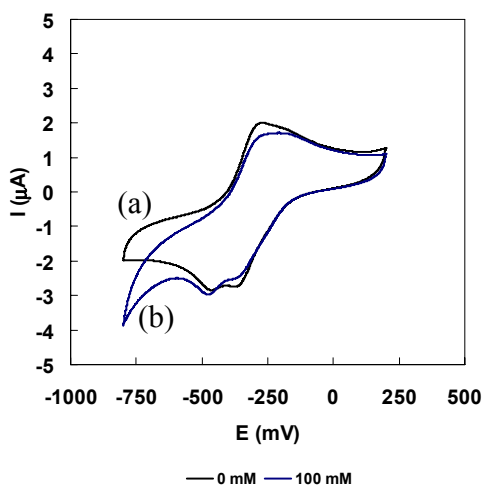


Figure S2. Cyclic voltammograms of $[\text{Cu}(\text{AMME-N}_3\text{S}_3\text{sar})]^{2+/+}$ (a) without EBiB and (b) with EBiB (100 mM) in DMSO. Complex concentrations are 1 mM and all voltammograms are recorded at 50 mV/s scanning rate in 0.1 M Et_4NClO_4 and are referenced to Ag/AgNO_3 .

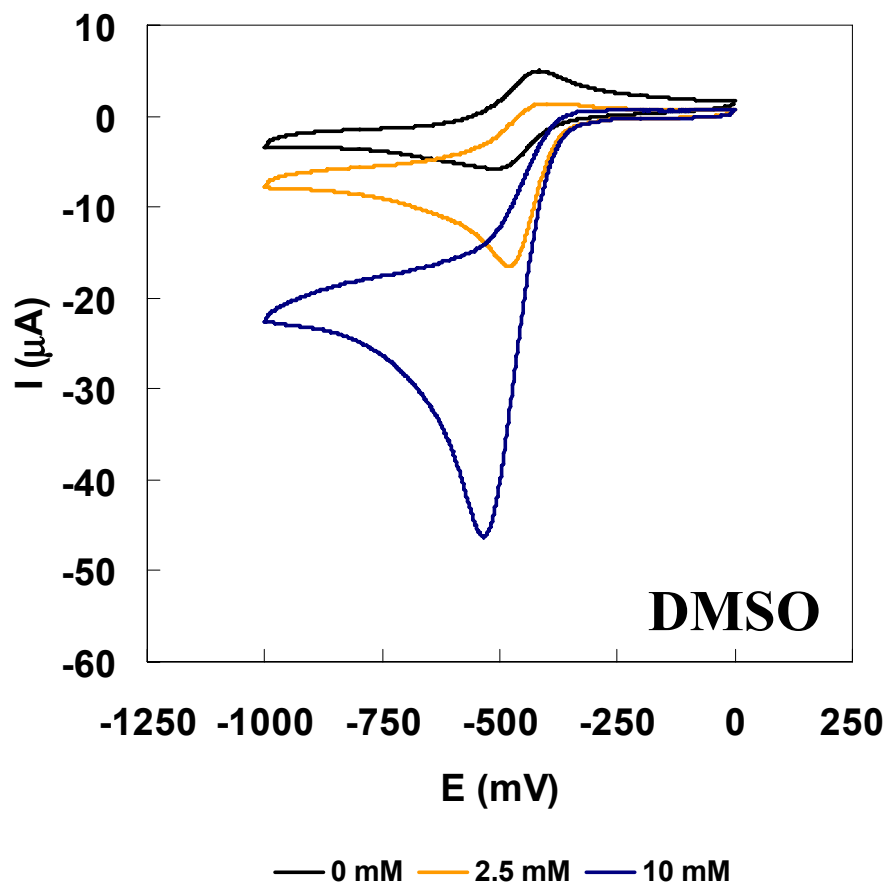


Figure S3: Cyclic voltammograms of $[\text{Cu}(\text{Me}_6\text{TREN})]^{2+/+}$ with varying concentrations of EBiB (0 - 10 mM) in DMSO. Complex concentrations are 1 mM and all voltammograms are recorded at 100 mV/s scanning rate in 0.1 M Et_4NClO_4 and are referenced to Ag/AgNO_3 .

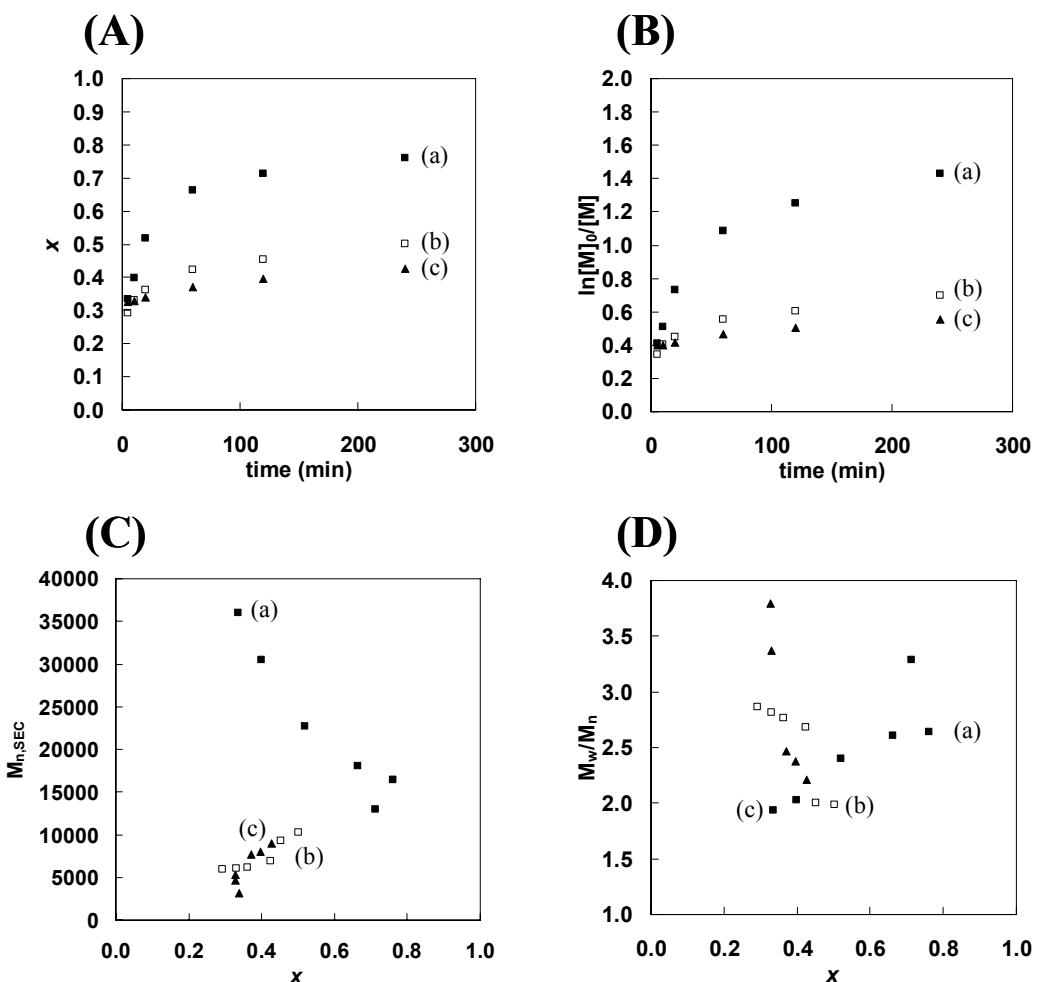


Figure S4: Kinetic data for the polymerization of methyl acrylate (3.67 M) in DMSO (9.36 M) at 25 °C with EBiB (1.83×10^{-2} M), CuBr (1.83×10^{-2} M) and AMME-N₃S₃sar. (A) conversion versus time, (B) $\ln[M]_0/[M]$ versus time (C) number-average molecular weight ($M_{n,SEC}$) versus conversion, and (D) polydispersity index versus conversion. The concentration ratios of reactants [MA]/[EBiB]/[CuBr]/[AMME-N₃S₃sar] are (a) 200/1/1/1, (b) 200/1/1/2, and (c) 200/1/1/3

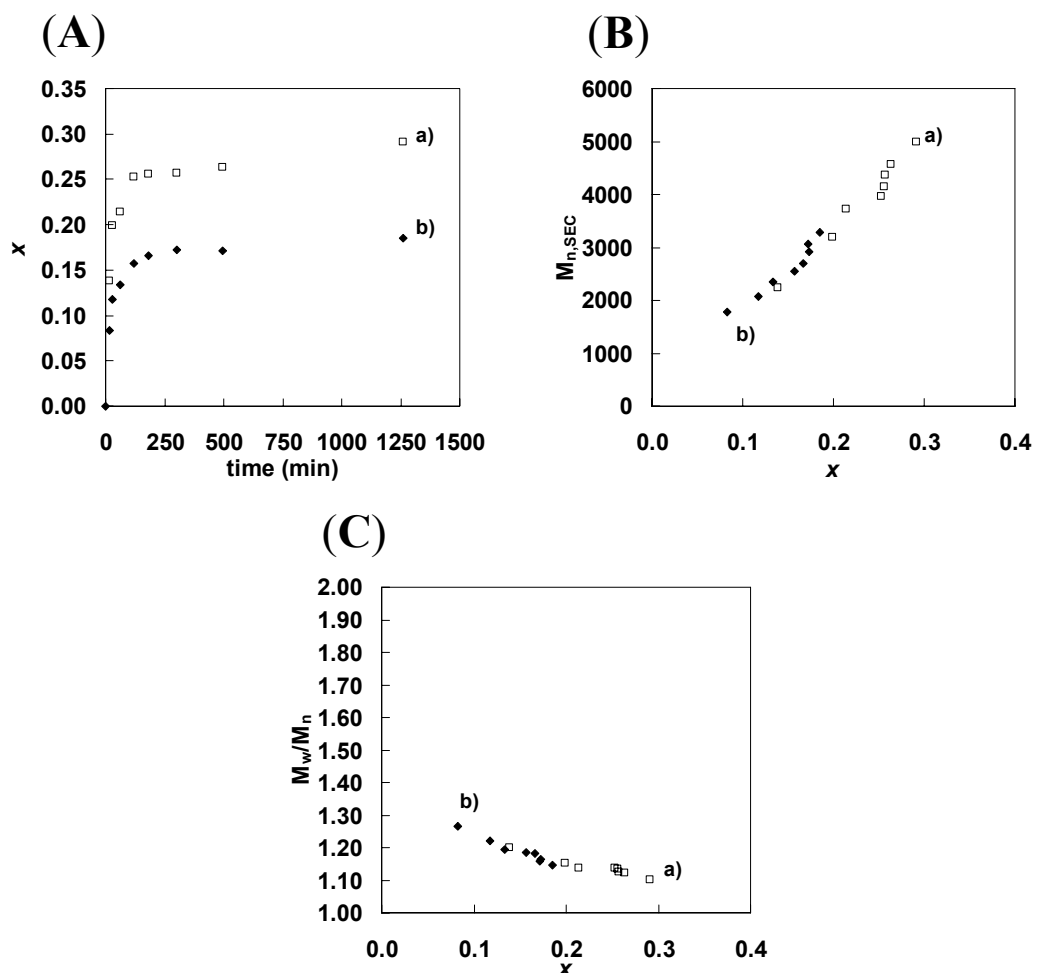


Figure S5: Kinetic data for the polymerization of methyl acrylate (3.67 M) in DMSO (9.36 M) at 25 °C with EBiB, MCEBTTC, CuBr and either AMME-N₃S₃sar or Me₆TREN where [MA]/[RAFT]/[EBiB] = 200/1/0.1. For all reactions, [EBiB]/[CuBr]/[ligand] = 1/1/1. (A) conversion vs time, (B) number-average molecular weight (M_{n,SEC}) vs conversion, and (C) polydispersity index vs conversion. Curves (a) CuBr/AMME-N₃S₃sar (b) CuBr/Me₆TREN.

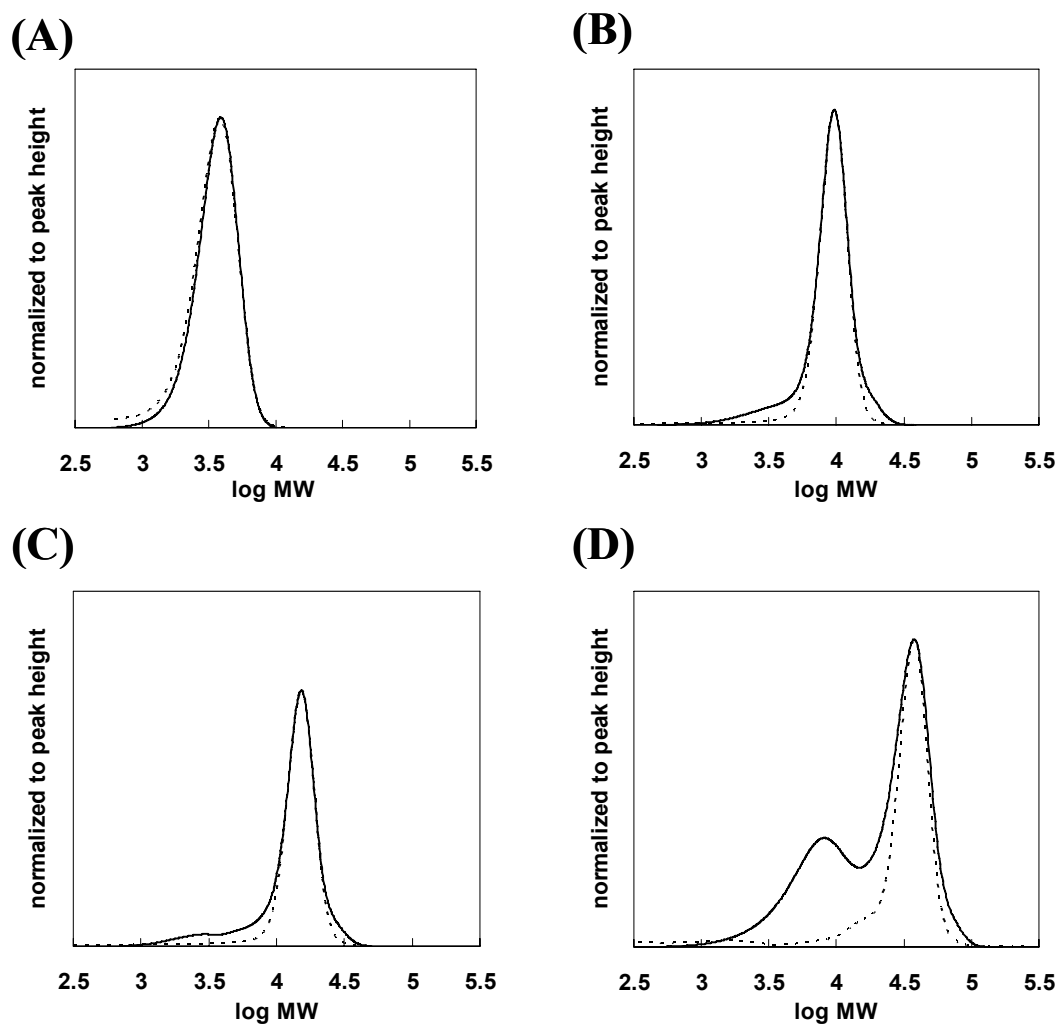


Figure S6: Dual detector Size Exclusion Chromatograms of MCEBTTC mediated polymerization of methyl acrylate (3.67 M) in DMSO (9.36 M) at 25 °C with EBiB, MCEBTTC, CuBr and Me₆TREN at various ratios of initiator (— represents refractive index, --- represents UV absorbance at 306.6 nm). The concentration ratios of reactants [MA]/[EBiB]/[CuBr]/[Me₆TREN]/[MCEBTTC] are (A) 200/0.1/0.1/0.1/1, (B) 200/1/1/1/1, (C) 200/1/1/1/0.5, and (D) 200/1/1/1/0.1

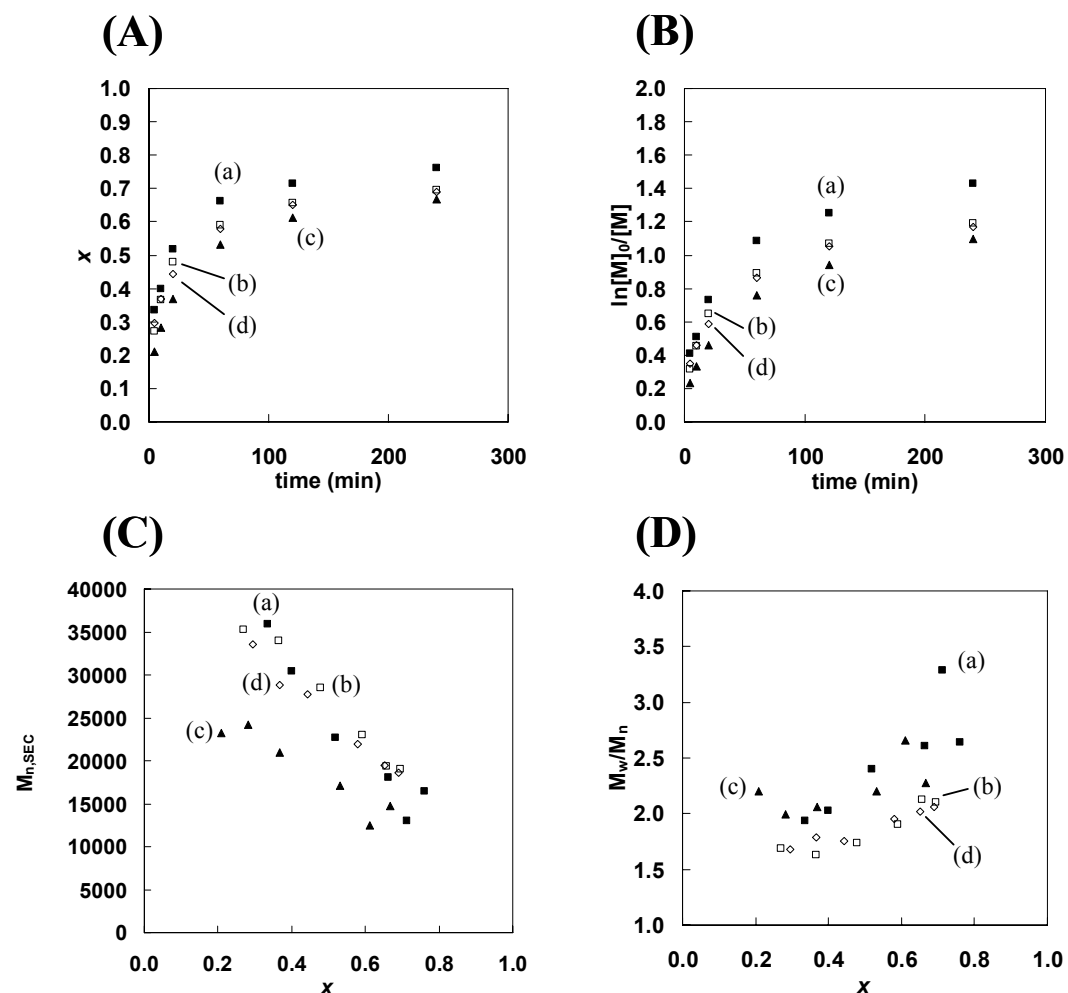


Figure S7: Kinetic data for the polymerization of methyl acrylate (3.67 M) in DMSO (9.36 M) at 25 °C with EBiB (1.83×10^{-2} M), CuBr, $[\text{Cu}(\text{AMME-N}_3\text{S}_3\text{sar})]\text{Br}_2$ and AMME-N₃S₃sar. (A) conversion versus time, (B) $\ln[\text{M}]_0/[\text{M}]$ versus time (C) number-average molecular weight ($M_{n,\text{SEC}}$) versus conversion, and (D) polydispersity index versus conversion. The concentration ratios of reactants $[\text{MA}]/[\text{EBiB}]/[\text{CuBr}]/[\text{AMME-N}_3\text{S}_3\text{sar}]/[\text{Cu}(\text{AMME-N}_3\text{S}_3\text{sar})]\text{Br}_2$ are (a) 200/1/1/1/0, (b) 200/1/1/1/0.05, (c) 200/1/1/1/0.1, and (d) 200/1/1/1/0.3